Determination of Nanoparticle Surface Coatings and Nanoparticle Purity Using Microscale Thermogravimetric Analysis

ARTICLE *in* ANALYTICAL CHEMISTRY · JANUARY 2014

Impact Factor: 5.64 · DOI: 10.1021/ac402888v · Source: PubMed

4 AUTHORS, INCLUDING:

Elisabeth Mansfield
National Institute of Standards and Technology
37 PUBLICATIONS **425** CITATIONS

SEE PROFILE

analytical chemistry

Article

pubs.acs.org/ac

Determination of Nanoparticle Surface Coatings and Nanoparticle Purity Using Microscale Thermogravimetric Analysis

Elisabeth Mansfield,*[,†] Katherine M. Tyner,[‡] Christopher M. Poling,[†] and Jenifer L. Blacklock[†]

[†]Applied Chemicals and Materials Division, National Institute of Standards and Technology (NIST) Boulder, Colorado 80305, United States

[‡]Center for Drug Evaluation and Research, Food and Drug Administration, Silver Spring, Maryland 20993, United States

ABSTRACT: The use of nanoparticles in some applications (i.e., nanomedical, nanofiltration, or nanoelectronic) requires small samples with well-known purities and composition. In addition, when nanoparticles are introduced into complex environments (e.g., biological fluids), the particles may become coated with matter, such as proteins or lipid layers. Many of today's analytical techniques are not able to address small-scale samples of nanoparticles to determine purity and the presence of surface coatings. Through the use of an elevated-temperature quartz crystal microbalance (QCM) method we call microscale thermogravimetric analysis, or μ-TGA, the nanoparticle purity, as well as the presence of any surface coatings of nanomaterials, can be measured. Microscale thermogravimetric analysis is used to determine the presence and amount of surface-bound ligand coverage on gold nanoparticles and confirm the presence of a poly(ethylene glycol) coating on SiO_2 nanoparticles. Results are compared to traditional analytical techniques to demonstrate reproducibility and validity of μ-TGA for determining the presence of nanoparticle surface coatings. Carbon nanotube samples are also analyzed and compared to conventional TGA. The results demonstrate μ-TGA is a valid method for quantitative determination of the coatings on nanoparticles, and in some cases, can provide purity and compositional data of the nanoparticles themselves.

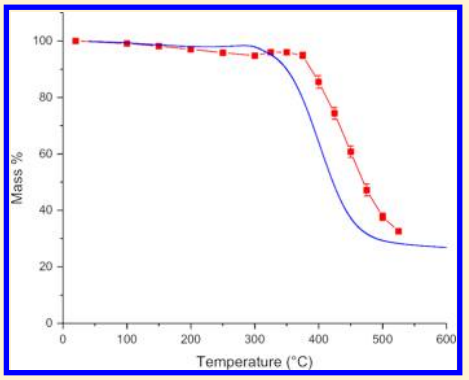

Physicochemical characterization of nanomaterials is a complex problem because it often requires multiple analytical techniques to provide all the relevant data to understand nanoparticle morphology and composition. Surface composition on nanomaterials, in particular, can be an ever-changing feature because a nanomaterial's surface composition can change because of exposure to biological fluids or other environmental factors. In cases where the surface is intentionally modified, the challenge is often ensuring that coverage of the particle is complete, uniform, and of the correct composition.[1,2] One of the greatest challenges in characterizing nanomaterials is understanding the properties of the surface composition, because the surface of the nanomaterial will often dictate its interactions with the environment.[3] There is therefore a growing need to accurately characterize the surfaces and coatings of nanoparticles as it is necessary prior to their desired applications.

Characterization of nanomaterials and their coatings is accomplished by use of a variety of analytical techniques, all of which have advantages and disadvantages. One common method for characterizing nanoparticle surface coatings is electron microscopy, including scanning electron microscopy (SEM) and transmission electron microscopy (TEM). Electron microscopy can be used to evaluate the presence of nanoparticle coatings on dried nanoparticles and can be paired with secondary detectors to allow for elemental composition analysis.[4] While electron microscopy can be used to measure particle sizes and visually inspect coating uniformity, it can require tedious work to understand the data, prepare the sample for imaging, and image enough nanoparticles to gain meaningful statistics.[5] Atomic force microscopy (AFM) can also be used to examine nanoparticle morphology but requires analysis of many particles to get statistical information.[6] Dynamic light scattering (DLS) is a common technique for establishing nanoparticle size and can handle large volumes of nanomaterials. DLS measures hydrodynamic diameter of the nanomaterial and the coating, which can be dependent on factors (i.e., such as sample concentration, salt concentration of suspending media, and electrical double layer).[7] Other methods to look at nanoparticle size include field flow fractionation (FFF),[8] nanoparticle tracking analysis (NTA), and UV−visible absorbance.[9] Nuclear magnetic resonance (NMR),[2] inductively coupled plasma emission spectrometry (ICP-OES),[10] and fluorescence spectrometry[1] can also be used to provide information beyond particle size, but interpretation of results may be difficult, as often the nanoparticle-ligand interaction can lead to inaccurate results. Additional surface analytical techniques, such as X-ray photoelectron spectroscopy (XPS), time-of-flight−secondary ion mass spectrometry (TOF-SIMS) and diffusion ordered spectroscopy-nuclear magnetic resonance (DOSY-NMR) are common methods to analyze surface

Received: September 10, 2013
Accepted: January 8, 2014
Published: January 8, 2014

coatings on nanoparticles. For all nanoparticle samples, it is necessary to provide a complete picture by using many techniques to provide complementary information.

Thermogravimetric analysis (TGA) is a straightforward analytical technique that typically requires no special sample preparation beyond drying of the sample. Past research has shown that TGA can be reliably used to evaluate the purity of and characterize nanomaterials.[11] For thermogravimetric analysis, materials are heated to elevated temperatures while monitoring the mass of the sample, which yields the decomposition curve. Analysis of the decomposition curve yields the oxidation temperature and residual mass of the sample. The oxidation temperature, as defined here, is the temperature at which the bulk of the material decomposes. For carbon-based materials, the residual mass, or ash content, is the remaining mass of the sample after decomposition. For nanomaterials, residual mass could be due to inorganic nanomaterials, residual metal catalysts from synthesis, or impurities within the sample. A drawback on the use of TGA is that a single sample can consume several milligrams of the nanomaterial, which, depending on the material in question, can result in prohibitively large cost to gain meaningful statistics. Measuring small, laboratory-scale samples, thin films, and samples with minor modifications in surface or bulk chemistry are at or below the limits of conventional TGA instrumentation. A method known as microthermogravimetric analysis (μ-TGA) uses the same thermal decomposition principle as TGA, but uses samples on the order of 1 μg and can detect mass changes less than a nanogram, thus greatly improving the detection limits of conventional TGA.[12]

In μ-TGA, a quartz crystal microbalance (QCM) is used to detect the mass of nanomaterials via piezoelectricity, which is sensitive to mass changes on the order of nanograms. When nanomaterials are deposited on the active area of the QCM electrode, the resonant frequency is dampened. The shift in the resonant frequency can be related to a shift of mass by using the equation developed by Sauerbrey.[13] Once the nanoparticle sample is deposited, the QCMs are heated in a box-furnace at increasing intervals with the frequency of the QCM being read at the end of the interval, thus simulating the effect of TGA and yielding a decomposition curve from which materials can by evaluated. The advantage of μ-TGA is that micrograms, instead of milligrams, of mass are required to obtain results. μ-TGA has been shown to be representative of the results one can achieve with TGA decomposition but has not been well established for the analysis of nanomaterials and their coatings.[11,14]

Here, μ-TGA is used to analyze a variety of nanoparticles to demonstrate how this technique could be applied to evaluate the decomposition of nanomaterials and their coatings. This work specifically outlines how this new μ-TGA technique can be used to address concerns that arise in nanoparticle samples, such as small volume and validates the results against other analytical instrumentation. Carbon nanotubes are measured by microscale TGA to give oxidation temperatures of the material, as well as residual mass (which is due to catalyst after the decomposition of carbon is complete). These results are compared to conventional TGA measurements to establish accuracy of the technique. Reproducibility of the μ-TGA technique is established, and limitations of the technique are also identified, from the analysis of SiO_2 nanoparticles with and without poly(ethylene glycol) coatings. Finally, complex nanoparticles, such as layer-by-layer coated gold nanoparticles are analyzed as an example of how microscale TGA can help in evaluating nanoparticle coatings.

EXPERIMENTAL SECTION

Materials.[15,16] Single-wall carbon nanotubes (SWCNTs) were obtained from NIST (Standard Reference Material (SRM) no. 2483: Single-Wall Carbon Nanotube soot) or produced from a commercial manufacturer using an arc discharge process. The arc-discharge-produced materials are considered to be 12+ % by weight carbon nanotubes and approximately 25% by weight metal catalyst particles. Ludox SM30 colloidal silica suspension (30 wt % in water, Sigma-Aldrich) was characterized prior to use and then coated with polyethylene glycol (PEG). NIST SRM 8012 gold nanoparticles, nominal 30 nm diameter, were used as the starting material for layer-by-layer coated nanoparticles. Poly(L-lysine) (PLL) is commonly used for DNA compaction and cell transfection. Poly-L-lysine (high molecular weight, was used for these experiments with a molecular weight of 70 000−150 000 g/mol) and DNA, gWiz High-Expression GFP plasmid (6.7 kb) purchased from Aldevron (Fargo, ND) was used without purification.

SiO_2−PEG Synthesis. Deionized water (0.5 mL) and 9.5 mL of 200 proof ethanol were placed in a 20 mL plastic vial. Contents were shaken to mix, and the pH was adjusted with 1 mol/L HCl to a pH of 5.5. In a second 20 mL plastic vial, a stir bar and 2.5 mL of the prepared acidic ethanol solution was added. Ludox SM30 (300 μL) was added dropwise into the solution while stirring (625 rpm). The solution turned cloudy upon addition of the silica nanoparticles. In a third 20 mL plastic vial, 0.1 g of mPEG−silane MW 5000 (Nanocs) was dissolved in 2.5 mL of 200 proof ethanol and 0.5 mL of deionized water. The solution was vortexed until clear. The solution was dropped into the stirred nanoparticle solution slowly over 2 min. The vial was capped and the solution was stirred for 22 h. At the end of the 22 h, the solution was milky-white with material visible at the top of the vial. The contents of the vial were dispersed by shaking and then transferred into 50 000 molecular weight cutoff dialysis tubing. The nanoparticles were dialyzed against deionized water for 2 days with 6 water changes to remove excess ligand. The purified sample was milky white with some visible precipitate. TEM images before and after coating revealed individual particles with a core size of approximately 7 nm (6−13 nm particle range)both before and after coating, with some agglomerates present. An increase in particle size with coating was validated using DLS.

Layer-by-Layer Coated Gold Nanoparticle Synthesis. LbL films were deposited onto citrate-stabilized gold nanoparticles in a solution of 10 mmol/L of bovine serum albumin (BSA) along with 10 mmol/L of PLL or 100 mmol/L of DNA. Because of the gold nanoparticles, (AuNP) inherent negative charge, a layer of PLL was first deposited on the nanoparticles. NIST stock AuNP solution (0.2 mL) was added to 2 mL of either PLL of DNA solution. After the addition of AuNPs to either PLL or DNA, the particles were left to sit for 5 min with gentle shaking. After 5 min, the solution was placed in the centrifuge for 10 min until the particles condensed at the bottom of the vials. Next, the remaining solution was taken out and 2 mL of the 100 mmol/L solution of DNA were added to the particles. The processes were repeated until 4 layers were deposited on the AuNP (PLL-DNA-PLL-DNA). After the fourth layer was deposited and the particles were placed in a

dx.doi.org/10.1021/ac402888v | Anal. Chem. 2014, 86, 1478−1484

centrifuge, the coated AuNP were left to sit in 10 mmol/L of BSA, which prevented aggregation.

Quartz Crystal Microbalance (QCM) Analysis. Ten megahertz AT-cut quartz crystals (1.37 cm diameter) with chromium/gold electrodes (0.51 cm in diameter) were mounted in spring-loaded fixtures to minimize edge clamping and then analyzed with a commercial impedance analyzer. The resonant frequency of the uncoated QCM was measured. Then, samples were applied from dispersions that were drop-cast (2 μL per drop) onto the quartz crystal surface by use of a pipet. Each drop was allowed to dry for 10 min on a hot plate at 75 °C to remove water. The frequency of the coated QCM was read after sample deposition. This initial measurement provides the initial concentration of particles (mg/mL) from the test solution. Carbon nanotube material was deposited by spray-coating prepared mixture in chloroform onto the crystal face with an air gun. The chloroform evaporated rapidly at ambient conditions following deposition. Other nanomaterials were drop cast from aqueous dispersions and dried prior to use. In the case of gold nanoparticles, a spin-on glass layer was deposited and cured prior to adding the nanoparticles. This glass coating prevented the gold nanoparticles from interacting with the gold electrode at elevated temperatures and improved reproducibility. Deposition and drying conditions were evaluated for each new material deposited on the crystal face to ensure film uniformity and validity of the Sauerbrey equation as described previously.[12]

To heat the materials to the appropriate test temperatures, the QCMs were removed from their spring-loaded fixtures and placed on an aluminum oxide tray. A box furnace with an integrated temperature controller was employed for all heating experiments. Each microbalance was heated at a rate of 10 °C/min to the desired temperature, held isothermally for one minute, and then cooled back to room temperature. This heating rate has previously been used for thermal analysis of nanomaterials and found to be an appropriate match for the thermal decomposition of the materials used here.[11,12,14,17] Once the materials reached ambient temperature, the resonant frequency of each QCM was measured with the impedance analyzer.

For all experiments, control QCM oscillators (i.e., without coatings applied) were heated alongside the test materials to compensate for stresses induced in the quartz by thermal cycling. The average change in resonant frequency of the control crystals for each thermal profile was used as the correction factor following the previously published method.[12]

Calculation of Mass. Frequency measurements were related to mass changes by use of the Sauerbrey equation,[18,19] as follows:

$$\Delta f = \left[\frac{-2f_o^{\,2}}{A\sqrt{\rho_q \mu_q}}\right]\Delta m \qquad (1)$$

where A is the active area (here, A = 0.2043 cm^2), ρ_q is the density of quartz (ρ_q = 2.48 g/cm^3), μ_q is the shear modulus of quartz ($\mu_q = 2.947 \times 10^{11}$ g/cm^3·s^2), f_o (MHz) is the resonant frequency of the QCM, and Δf (Hz) is the frequency shift correlating to the change in mass, Δm. The resonant frequency of each QCM was measured initially (f_o), after application of coating, and after each successive heating. Minor changes in the resonant frequency were observed for control QCMs because of stresses induced by successive heating. Stresses due to thermal heating have been well documented to have an effect on the frequency of quartz crystal microbalances.[20] In many cases, to account for temperature effects, dual QCM geometries have been used, in which one electrode functions as a reference.[21,22] To account for thermal stresses here, a correction factor was applied based on the average change in baseline frequency for a control QCM because of a particular heating profile. This approach is similar to other reference crystal methods discussed in the literature successfully used for correcting for thermal stresses.[22] As previously noted,[12] this heating correction became significant at temperatures above 425 °C, where thermal stresses become more significant as the Curie temperature of quartz (573 °C) was approached. In addition to correction for thermal stresses, adsorbed water was accounted for in those instances in which substantial loss of mass was observed at 100 °C. When this mass loss exceeded 5% of the initial mass, the coating mass was corrected for the adsorbed water, and the mass percent loss for the QCM measurements was recalculated based on the water-corrected frequency shift. Examples of this correction can be found in previous publications.[12]

Thermogravimetric Analysis (TGA). Sample masses were approximately 1 mg for SiO_2 nanoparticle materials and 5 mg for carbon nanotube materials. For the carbon nanotube measurements, samples were placed in 100 μL ceramic pans and equilibrated to 40 °C in the TGA, and then heated at a rate of 10 °C/min to 800 °C, unless otherwise noted. For the materials tested here, no oxidation was found above 800 °C and heating rates of 10 °C/min yielded the most reproducible results. During the sample measurement, air was introduced to the samples at a rate of 25 mL/min to maintain an oxidizing environment around the sample. Air flow of 25 mL/min was found to be sufficient to remove oxidation products without introducing buoyancy effects. For the SiO_2−PEG nanoparticles, 25 μL of the stock solutions were placed in aluminum pans, resulting in a mass of 24.8 mg, which was reduced to 94 μg of sample after water was removed by heating the sample to 100 °C. Data were smoothed to provide more clarity for plots, as a mass of 94 μg was below the reported sample limits of the instrument (1 mg). For the coated SiO_2 nanoparticles, the temperature was ramped at 2 °C/min to 550 °C. For the uncoated nanoparticles, 25 μL of the stock solution was placed in an aluminum pan for 1 °C/min to 550 °C. The NIST Standard Reference Material (SRM) no. 2483: Single Wall Carbon Nanotube soot has a reported residual mass of 7.09 ± 0.33% and an oxidation temperature of 482.2 ± 1.2 °C. Extensive purity of the arc discharge material is reported elsewhere.[30]

RESULTS AND DISCUSSION

Microscale thermogravimetric analysis (μ-TGA) allows for 1000-fold less sample mass than conventional TGA measurements. Previously, the application of this new microscale TGA technique was demonstrated using well-studied materials (aluminum oxide, carbon black), as well as nanomaterials (carbon nanotubes).[12] Nanomaterial analysis can benefit from the use of microscale techniques, as many materials are not made in high quantities or are prohibitively costly to analyze. A variety of nanoparticles were analyzed to demonstrate to evaluate how μ-TGA could be applied to particles of different core compositions (metals, carbon particles) with surface coatings (polymers, biological molecules), to determine

dx.doi.org/10.1021/ac402888v | Anal. Chem. 2014, 86, 1478−1484

reproducibility the limits of the μ-TGA technique, and to demonstrate the limitations of the technique.

Carbon nanotube samples are analyzed by TGA to provide a measure of purity and composition of the sample[11] by looking at oxidation temperatures and residual mass. Single-wall carbon nanotube samples were analyzed using μ-TGA and the results were compared to conventional TGA to ensure accuracy (Figure 1). When oxidizing carbon nanotubes, three major components can be identified. At low temperatures (200−300 °C), amorphous carbons oxidize and then are followed by nanotubes (300−500 °C). The mass that remains after heating beyond when the carbon decomposes is called the residual mass (M_{res}) and is attributed to catalyst particles left over from the synthesis process, as well as any oxidation products of the catalyst. Carbon nanotube samples for μ-TGA were coated onto QCMs by use of a spray coating process to ensure a uniform, thin-film on the surface of the QCM. The material was heated to 100, 150, 200, 250, 300, and every 25 °C after that up to 525 °C. By decreasing the spread of data points to every 25 °C, the full oxidation of the carbon nanotubes could be captured. The μ-TGA results follow those of the TGA curve closely, ending at approximately the same residual mass values as observed in the conventional TGA. Figure 1A shows the μ-TGA results obtained for NIST SRM 2483, a single-wall carbon nanotube soot, as compared to conventional TGA. At low temperatures, the mass fluctuates around 100%, presumably because of associated water with the material. Because the μ-TGA measurement is not continuous, water can be associated with the material after heating and with detection limits of a QCM are on the order of a nanogram, the measurement is very sensitive to humidity. After heating to 300 °C, the excess water seems to be driven off and the material initiates decomposition around 425 °C in both the conventional and microscale instrument. The material continues to decompose with μ-TGA measurements closely following those of the bulk mg-scale measurements. Oxidation of the catalyst particles is seen after 525 °C in the μ-TGA measurements, leading to dramatic mass changes (not shown). At 575 °C, the μ-TGA has a residual mass of 16.75% ± 2.01% (±1 s.d.) in comparison to the 7.17% in the conventional TGA. Figure 1B shows another single-wall carbon nanotube material analyzed using μ-TGA. This material, in contrast to the NIST SRM 2483, is of very poor quality with approximately 36% metal. The μ-TGA results again closely follow that of the conventional TGA, demonstrating μ-TGA as a reliable method for analysis of carbon nanotubes similar to conventional TGA with a 1000-fold decrease in sample volume. With the shift of oxidation temperature of the SWCNT, the given mass % remaining at a temperature can be approximately 20% different between samples while the shapes of the thermograms remain the same. At 525 °C, the residual mass in the μ-TGA is 32.59% ± 0.6% in comparison to the conventional TGA result of 27.22%. This shift in oxidation temperature could be due to differences in sample volumes and heating environments, as previously reported.[12] Uniformity of heating is important, and the sprayed-on microscale samples are expected to be less packed than those in a crucible in the conventional TGA. The smaller sample may help eliminate mass and heat transfer within the sample, eliminate secondary reactions that enable self-heating or self-cooling and allow for more reproducible exposure to the oxidizing atmosphere. μ-TGA is relevant for newly purified materials in which single chiralities of carbon nanotubes are isolated, but not in significant enough volume for conventional TGA.

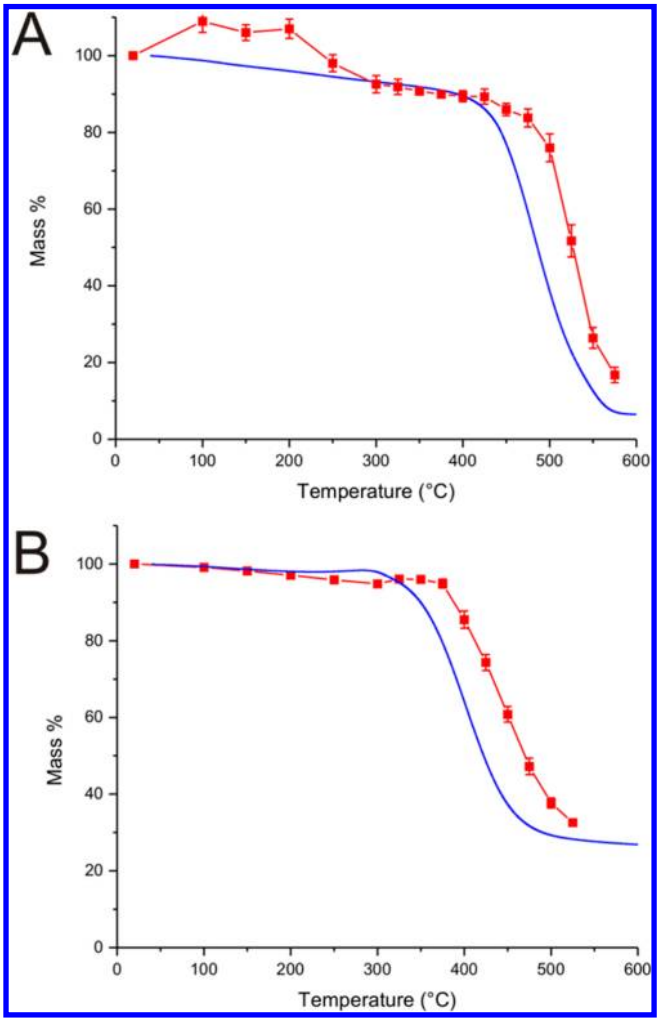

Figure 1. Mass percent versus temperature thermograms for μ-TGA (red) and conventional TGA instruments (blue). (A) NIST SRM 2483 single-wall carbon nanotube soot and (B) a high metal content nanoparticle sample.

The reproducibility of the μ-TGA technique was tested by analyzing the same nanoparticle sample twenty-five times. Without reproducibility in heating batches, the μ-TGA analysis could not be used for analytical analysis of nanoparticle coatings. Silica nanoparticles, coated with polyethylene glycol (SiO_2−PEG) were coated onto QCMs by drop-casting a suspension and allowing it to dry to a film. QCMs were heated to 100, 200, 250, 300, 400, 500, and 600 °C (Figure 2A). Initial deposited mass of approximately 10 μg per sample was recorded at room temperature (22 °C). The average mass percent, standard deviation, and relative standard deviations (RSD %) are shown in Table 1. Because the sample exhibited very little effect from adsorbed water (<1 mass % change at 100 °C), no water correction was used for these sample runs. As the sample was heated, the degradation of PEG started immediately and continued until the 400 °C mass reading, with the major transition happening between 200 and 400 °C. At the 500 °C measurement, the mass increased from the measurement at 400 °C. This is presumably because of oxidation of the SiO_2 nanoparticle after the nanoparticle coating has been decomposed fully. For most temperatures, the relative standard deviation is below 4% of the average mass percentage, which is

dx.doi.org/10.1021/ac402888v | Anal. Chem. 2014, 86, 1478−1484

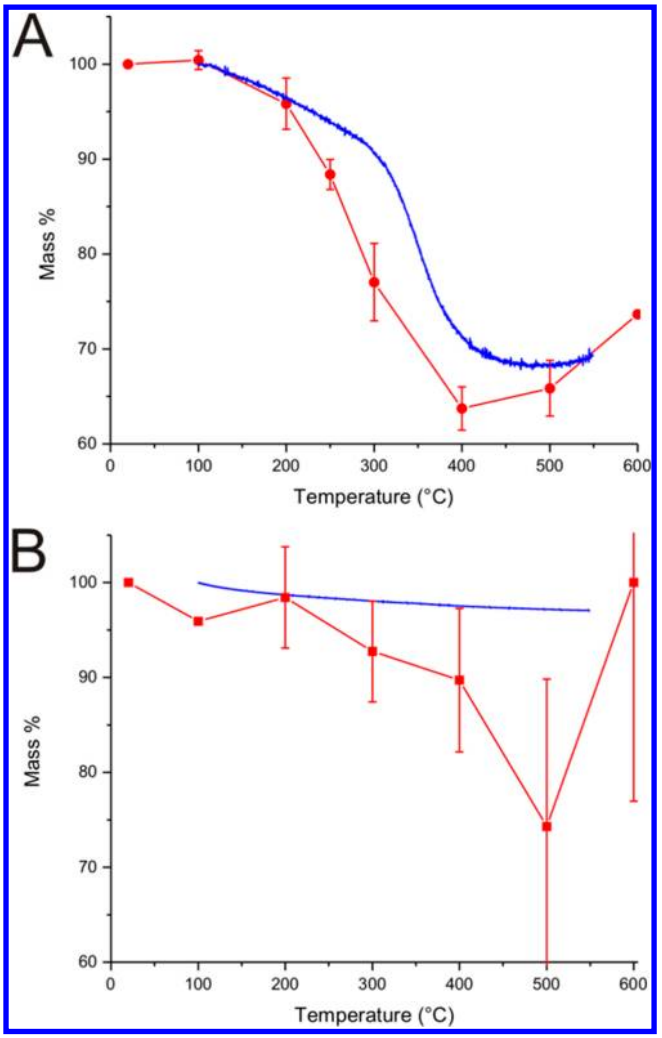

Figure 2. (A) Mass % versus temperature thermogram of SiO_2−PEG (n = 25) nanoparticle samples evaluated using μ-TGA (red) as compared to a conventional TGA measurement (blue). (B) Mass % versus temperature thermogram of SiO_2 (n = 8) nanoparticle samples evaluated using μ-TGA (red) as compared to a conventional TGA measurement (blue).

comparable to other measurements of residual mass by TGA. At 300 °C, the material is undergoing the major transition for the PEG coatings. At 500 °C, the error is also large, as the material is undergoing oxidation due to increased exposure to air without the surface coating. The oxidation of Si to form SiO_2 at elevated temperatures in bulk[23] and in nanoparticle form[24] is well-known and would be expected to lead to an increase in mass as the oxide layer continued to grow. It is expected that the error in the measurements at 300 and 500 °C would be larger than those measurements where the material is not undergoing significant chemical changes. These chemical changes would be dependent on the exposure to the environment, packing of the material, integrity of the coating, and other factors that would impact the rate of reaction. The results of the conventional TGA analysis of the SiO_2−PEG particles shows the mass slowly declines from 100 to 350 °C, then has a large mass loss between 350 and 425 °C, which can be attributed to the PEG coating decomposition. The material mass is fairly steady after that, but begins to ramp up at about 550 °C again, most likely because of oxidation of the SiO2 nanoparticles. The TGA results were corrected for water at 100 °C, and the data were smoothed for clarity, as there was considerable noise in the measurement because of the small sample volume. The measured mass change for the PEG-coated SiO_2 is 31.79% at 500 °C by conventional TGA. The μ-TGA results show a mass loss of 34.1% ± 5.86% (average ±2 s.d.) at 500 °C. For the SiO_2−PEG samples, μ-TGA had a lower decomposition temperature, but is within error of the residual mass measurement. The oxidation temperature from the microscale TGA measurements is shifted to lower temperature (200 to 400 °C) where the major change in mass for the conventional TGA measurements is between 350 and 425 °C. This shift to lower temperatures has been seen previously[25] and is thought to be due to differences in the heating conditions between the two measurement systems and the cycles in temperature needed for μTGA.[12]

SiO_2 nanoparticles were also analyzed without PEG coatings. The results for SiO_2 nanoparticles as compared to SiO_2−PEG nanoparticles are also shown in Figure 2B as compared to the conventional TGA measurements. Upon heating, the mass of the uncoated SiO_2 nanoparticles decreases, with up to a 25% mass loss at 500 °C. At 600 °C, the sample mass for the uncoated SiO_2 nanoparticles increases dramatically, most likely because of oxidation of the silica at higher temperatures. In general, the uncertainty in the measurements for the uncoated SiO_2 nanoparticles is higher than that seen in the coated SiO_2−PEG samples, and the mass loss does not correlate with the conventional TGA measurements. Through the analysis of the two SiO_2 samples, one of the major limitations of the μ-TGA technique was identified. To analyze the nanoparticles, the sample must first be adhered to the surface of the QCM, and must remain adhered to the QCM surface throughout analysis. The interaction between the nanoparticles and the surface can be through many forces, including van der Waals forces and/or electrostatic interactions. The details of nanoparticle adhesion to surfaces have been discussed in the literature[26−28] and are not completely understood. Considering the larger error bars and increased mass loss, it is suggested that the uncoated SiO_2 nanoparticles may not adhere to the QCM surface as strongly as the coated SiO_2−PEG particles. Adhesion mechanisms between nanoparticles and polymers have been discussed for nanoparticle silver,[28] but less is known about SiO_2 nanoparticle adhesion to surfaces. It can be assumed that the polymer coating on the nanomaterial will have different adhesive forces, potentially increasing the interaction with the surface and changing the critical detachment force.[27] The larger uncertainty

Table 1. Average Mass Percent for Twenty-Five SiO_2−PEG Nanoparticle Samples

	temperature (°C)						
	20	100	200	250	300	400	500
average	100	100.427	95.8517	88.3802	77.0359	63.7344	65.859
SD	0	1.00103	2.69323	1.59153	4.08187	2.27163	2.92982
%RSD	0	0.99677	2.81038	1.80077	5.29866	3.56421	4.44862

dx.doi.org/10.1021/ac402888v | Anal. Chem. 2014, 86, 1478−1484

in uncoated SiO_2 measurements may be due to the decreased interactions at the QCM-nanoparticle interface, but could also be inaccurate due to incomplete coupling with the surface. Rigid, well-coupled thin films are necessary to relate changes in frequency to changes in mass with QCMs.[13] Fluctuations in the mass loss could also be due to contaminants on the SiO_2 sample as purchased.

Finally, more complex nanoparticles were analyzed using μ-TGA. Figure 3A shows μ-TGA results of layer-by-layer deposited coatings on NIST SRM 8012, a 30 nm gold colloidal nanoparticle. This complex particle is representative of a nanoparticle designed as a gene delivery system. Gold nanoparticles are thought to be biocompatible and are often used in nanomedicine applications. The first layer, poly-L-lysine (PLL), is a secondary amine, and has a pK_a close to that of the endosomal compartment within a cell. It is thought that this will allow for the particle to be introduced into the cell, and release the second layer of the particle, DNA, for efficient gene delivery to cells.[29] Samples were prepared with anywhere from one to four layers. The first deposited layer shows a mass remaining of 85.76 ± 14.1% (average ± 2 s.d.) at 400 °C. The second layer and third layer demonstrate masses at 400 °C of 69.75 ± 0.2% and 50.25 ± 12.8%, respectively. The observed lower standard deviation for the second layer is thought to be a result of uniform population of nanoparticles that are formed when the DNA is added. Finally, the last layer reflects a mass remaining of 43.64 ± 12.1%. This can be used with other results to determine particle coverage. Dynamic light scattering (DLS) results were used to compare to μ-TGA results. Figure 3B shows size measurements for the four samples analyzed in Figure 3A. The first deposition of PLL gives a size of 34 nm, up from the 30 nm reported sample size of SRM 8011. The second layer of DNA has an increase in diameter from layer 1 to 50 nm. DLS data on Layer 3 shows the particle remains consistent in size around 50 nm, and a small increase is observed to 60 nm is observed for layer 4. The increase in size from layer 2 (50 nm) to layer 4 (60 nm) is accompanied by an increase in the DNA content of the particle from 71.9 ± 5.0 to 104.1 ± 5.9 ng/μL, as measured by UV−visible spectrometry. Like other techniques, such as DLS or microscopy, the whole story is not told by just the μ-TGA results. Table 2 summarizes the results of the microscale TGA measurements, size as determined by DLS, and DNA content for the layer-by-layer gold nanoparticles. Using these data, it can be determined that there is a deposition of mass from the third PLL deposition step, although this does not necessarily correspond to an increase in the size of the nanoparticle, which reflects the DNA compaction properties of PLL previously reported in the literature.[29] The size increase from layer 3 to layer 4 is cross-verified as an increase in DNA by the UV−visible spectrometry results, confirming increased DNA content, as well as the increase in mass loss as measured by μ-TGA. For complicated nanoparticle systems such as multilayer nanoparticles or two-component particles, μ-TGA can provide additional information based on mass. The measured mass changes can reflect properties that may not be attainable from other measurements, like a DNA compaction in the above example. Further measurements with μ-TGA can be used to evaluate ligand deposition in nanoparticle systems that suffer from other measurement interferences, such as fluorescence quenching of ligands by metal-core nanoparticles (data not shown).

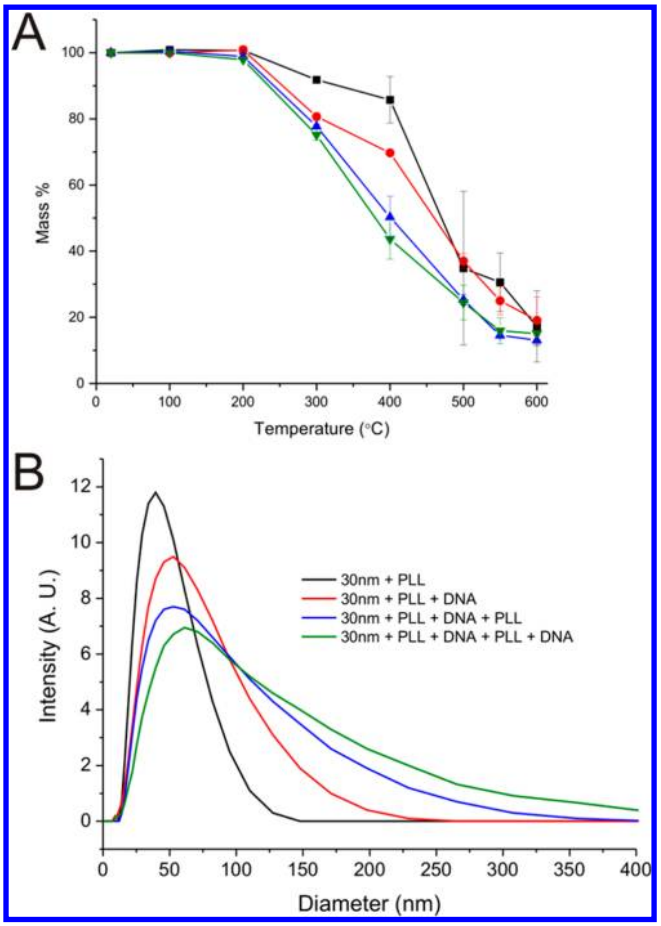

Figure 3. (A) μ-TGA mass % versus temperature thermograms of four layer-by-layer coated Au nanoparticle samples. (B) DLS results for particle intensity versus diameter for four layer-by-layer Au nanoparticle samples. In both, 30 nm AuNPs + PLL (black), 30 nm AuNPs + PLL + DNA (red), 30 nm AuNPs + PLL + DNA + PLL (blue), and 30 nm AuNPs + PLL + DNA + PLL + DNA (green).

Table 2. Mass Percent Remaining after Decomposition of All Layers, Size, and DNA Content for Layer-by-Layer Coated Gold Nanoparticles[a]

	mass percent remaining (%)	size (nm)	DNA content (ng/μL)
Au + PLL	85.76 ± 14.1	34	
Au + PLL + DNA	69.75 ± 0.2	53	71.9 ± 5.0
Au + PLL + DNA + PLL	50.25 ± 12.8	53	
Au + PLL + DNA + PLL + DNA	43.64 ± 12.1	61	104.1 ± 5.9

[a]Average with two standard deviations reported.

CONCLUSION

New techniques are needed to analyze nanoparticle populations, especially when conventional measurements are impractical. Thermogravimetric analysis can give information on nanoparticle coatings and purity of some nanoparticles. Moving toward microscale-TGA allows for the measurement of 1000-fold less sample mass than conventional TGA while yielding comparable results. Microscale TGA was established here as a viable measurement tool for nanoparticle analysis with repeatability on the order of typical TGA experiments, similar results to conventional TGA in terms of oxidation temperature

dx.doi.org/10.1021/ac402888v | Anal. Chem. 2014, 86, 1478−1484

and residual mass measurements in carbon nanotubes, and the ability to determine layer-by-layer coatings on a gold nanoparticle core or determine the ratio of two component particles by their different oxidation temperatures.

AUTHOR INFORMATION

Corresponding Author

*E-mail: elisabeth.mansfield@nist.gov. Phone: 303-497-6405. Fax: 303-497-5030.

Notes

This work is a contribution of NIST, an agency of the US government and is not subject to copyright in the United States. The findings and conclusions in this article have not been formally disseminated by the Food and Drug Administration and should not be construed to represent any Agency determination or policy.

The authors declare no competing financial interest.

REFERENCES

(1) Sperling, R. A.; Parak, W. J. *Phil. Trans. R. Soc. A* **2010**, *368*, 1333−1383.

(2) Zhang, B.; Yan, B. *Anal. Bioanal. Chem.* **2010**, *396*, 973−982.

(3) Nel, A. E.; Mädler, L.; Velegol, D.; Xia, T.; Hoek, E. M. V.; Somasundaran, P.; Klaessig, F.; Castranova, V.; Thompson, M. *Nat. Mater.* **2009**, *8*, 543−557.

(4) Caruso, R. A.; Susha, A.; Caruso, F. *Chem. Mater.* **2001**, *13*, 400−409.

(5) Postek, M. T.; Vladar, A. E. *Proc. SPIE* **2012**, *8378*, No. 837805.

(6) MacCuspie, R. I.; Rogers, K.; Patra, M.; Suo, Z.; Allen, A. J.; Martin, M. N.; Hackley, V. A. *J. Environ. Monit.* **2011**, *13*, 1212−1226.

(7) Hackley, V. A.; Clogston, J. D. *Measuring the Size of Nanoparticles in Aqueous Media Using Batch-Mode Dynamic Light Scattering*, NCL Joint Assay Protocol, PCC-1, version 1.1; National Institute of Standards and Technology: Gaithersburg, MD, 2010.

(8) Cho, T. J.; Hackley, V. A. *Anal. Bioanal. Chem.* **2010**, *398*, 2003−2018.

(9) Zook, J. M.; Long, S. E.; Cleveland, D.; Geronimo, C. L. A.; MacCuspie, R. I. *Anal. Bioanal. Chem.* **2011**, *401*, 1993−2002.

(10) Elzey, S.; Tsai, D.-H.; Rabb, S. A.; Yu, L. L.; Winchester, M. R.; Hackley, V. A. *Anal. Bioanal. Chem.* **2012**, *403* (1), 145−149.

(11) Mansfield, E.; Kar, A.; Hooker, S. *Anal. Bioanal. Chem.* **2009**, *396*, 1071−1077.

(12) Mansfield, E.; Kar, A.; Quinn, T. P.; Hooker, S. *Anal. Chem.* **2010**, *82*, 9977−9982.

(13) Sauerbrey, G. *Z. Phys.* **1959**, *155* (2), 206−222.

(14) Sebby, K. B.; Mansfield, E. *Eur. Cells. Mater.* **2010**, *20* (Suppl 3), 234.

(15) Certain commercial equipment, instruments, or materials are identified in this document. Such identification does not imply recommendation or endorsement by the National Institute of Standards and Technology, nor does it imply that the products identified are necessarily the best available for the purpose.

(16) The mention of commercial products, their sources, or their use in connection with material reported herein is not to be construed as either an actual or implied endorsement of such products by the Department of Health and Human Services.

(17) Hurst, K. E.; Van der Geest, A.; Lusk, M.; Mansfield, E.; Lehman, J. H. *Carbon* **2010**, *48*, 2521−2525.

(18) Mecea, V. M. *Sens. Actuators A* **1994**, *40*, 1−27.

(19) Lucklum, R.; Behling, C.; Hauptmann, P. *Sens. Actuators B* **2000**, *65*, 277−283.

(20) Mecea, V. M.; Carlsson, J. O.; Heszler, P.; Bârtan, M. *Vacuum* **1995**, *46* (7), 691−694.

(21) Bruckenstein, S.; Michalski, M.; Fensore, A.; Li, Z.; Hillman, A. R. *Anal. Chem.* **1994**, *66*, 1847−1852.

(22) Wang, D.; Mousavi, P.; Hauser, P. J.; Oxenham, W.; Grant, C. S. *Colloids Surf., A* **2005**, *268*, 30−39.

(23) Irene, E. A.; van der Meulen, Y. J. *J. Electrochem. Soc.* **1976**, *123* (9), 1380−1384.

(24) Holm, J.; Roberts, J. T. *Langmuir* **2007**, *23*, 11217−11224.

(25) Mansfield, E.; Quinn, T. P. *SPIE Newsroom* **2011**, DOI: 10.1117/2.1201102.003528.

(26) Carrillo, J.-M. Y.; Raphael, E.; Dobrynin, A. V. *Langmuir* **2010**, *26* (15), 12973−12979.

(27) Carrillo, J.-M. Y.; Dobrynin, A. V. *J. Chem. Phys.* **2012**, *137*, No. 214902.

(28) Joo, S.; Baldwin, D. F. *Nanotechnology* **2010**, *21*, No. 055204.

(29) Mann, A.; Richa, R.; Ganguli, M. *J. Controlled Release* **2008**, *125*, 252−262.

(30) Mansfield, E.; Kar, A.; Wang, C. M.; Chiartamonti, A. N. *Anal. Bioanal.* **2013**, *405* (25), 8207−8213.